Removal of Dyestuffs from Effluents onto Biochar

Subjects: Environmental Sciences | Green & Sustainable Science & Technology | Engineering, Environmental
Contributor: Prakash Parthasarathy , Samra Sajjad , , Gordon Mckay

Processing significant amounts of dye effluent discharges into receiving waters can supply major benefits to countries that are affected by the water crisis and anticipated future stress in many areas in the world. When compared to most conventional adsorbents, biochars can provide an economically attractive solution. In comparison to many other textile effluent treatment processes, adsorption technology provides an economical, easily managed, and highly effective treatment option.

effluents | dye removal | biochar | adsorption | dye absorption capabilities

1. Introduction

Dyestuffs color and pollute receiving waters, streams, and rivers as a result of inadequate processing of the industrial effluents by a variety of industrial applications including the food and beverage companies, paper and pulp processing, paint manufacturing, pharmaceutical processing, printing, textiles, dyeing, and printing [1]. Many dyes pose a grave danger to the water environmental ecosystem due to their chemical properties, with serious consequences for human health, animal, and plant ecosystems [2][3]. Aside from a limited number of studies indicating that specific dyes are toxic, the presence of dyestuffs into receiving waters reduces the photosynthetic process by inhibiting light from passing through [4]. During the degradation process, dyes consume the dissolved oxygen concentrations of the receiving water, therefore decreasing the water quality standards for aquatic species. This has detrimental visual aesthetic impacts which may result in health reproductive issues in fishes [5]. Specific dyes have a negative impact on the skin, kidneys, liver, reproductive system, heart, brain, and nervous system, and some may be carcinogenic or mutagenic.

Data on dyestuff effluent discharge volumes and production quantities are not readily available or recorded around the world. According to available data, 700,100 tons of dyestuffs are produced every year for 10,000 dyes. According to industry figures, the global dyestuffs produced yearly is 1.8 to 1.9 × 10^6 tons with more than 11,000 dye pigments applied primarily in the food, textile, cosmetics, leather, paper, and plastics industries [6]. Depending on the type of dyestuff and the process technology used, 1–10% of dye is not used in the dyeing process, indicating that significant amounts of dye are discharged to the water bodies via various means [7].

The majority of dyestuffs have specific characteristics such as chemically stable and light fastness [8]. Furthermore, the dye color reduces light penetration in streams and rivers, therefore reducing photosynthesis and dissolved oxygen content. They prevent a variety of chemical functions based on the material to which they are applied and

the color they impart (**Figure 1**). All of these properties are advantageous to the dye user and are enhanced by dyestuff manufacturers. However, the huge volumes of effluent makes the treatment of these dyes to comply with environmental effluent discharge standards very problematic. In addition, water can be colored in certain cases with dye concentrations as little as 1 ppm. The majority of dyeing applications employ copious amount of water during the dyeing, washing, and rinsing stages [9][10].

Figure 1. (**A**) Dye house discharge. (**B**) River quality affected by dyestuffs.

2. Dye Classifications

Dyes are colored molecules or ions that can be applied to a wide range of materials including food, beverages, and textiles in solution or as a dispersion. Most dyes have a high-water solubility, and often contain a sulfonic acid group, usually in the form of a sodium salt, which is responsible for the solubility of many water-soluble dyestuffs [11]. Dye colors are created by chemical groups absorbing light of various wavelengths in the visible region of the spectrum. Different unsaturated chemical groups on chromophores promote this key distinguishing property. **Figure 2** depicts the more common ones.

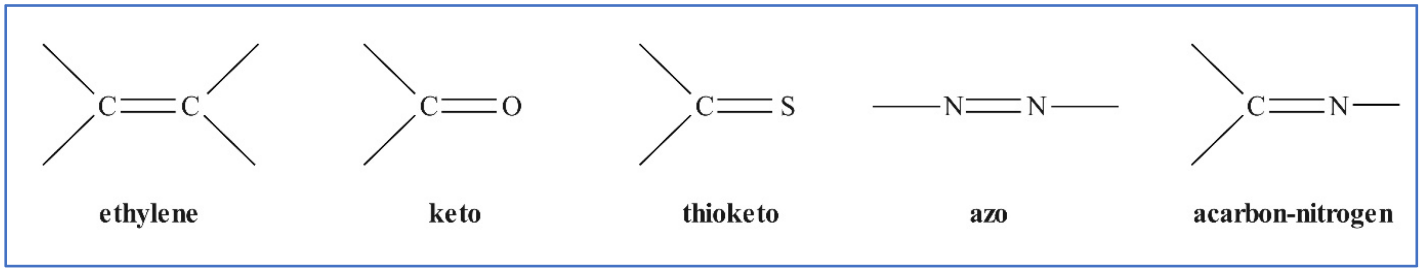

Figure 2. Color-producing chromophores or groups.

Auxochromes are groups that can also enhance the water solubility and improve the dye absorption potential for adsorbing material; examples include substituted sulfonic, hydroxyl, carbonyl, or amino groups. Dyes can be classified based on their chemistry or their types of application. As a result, the chemical structure and type of dye must be a primary consideration in determining which dye wastewater process treatment technology should be applied for effluent removal, as well as determining what adsorbent properties are required for the adsorption of the specific dyestuff type.

2.1. Reactive Dyes

Reactive dyes are used extensively in the dyeing of cellulosic textile fibers, namely, flax and cotton. Due to their high adhesion to a substrate, they can also be used to dye linen, viscose, and silk [12][13]. These reactive compounds in the dye can form chemical bonds with textile uptake of fibers. The uptake of the dichlorotriazine type of reactive dye which becomes attached to the cellulose fiber by displacing the chloride grouping is depicted in the mechanistic schemes below. One or both chlorides may be present. **Figure 3** and **Figure 4** show the typical dye uptake mechanisms for dyeing cellulosic materials.

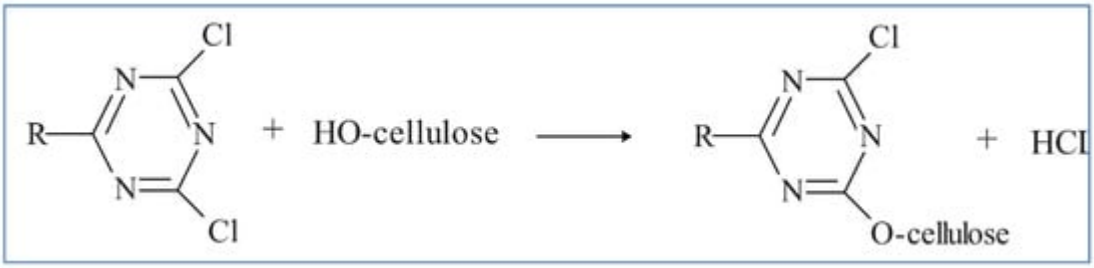

Figure 3. Typical mechanisms for dyeing cellulose.

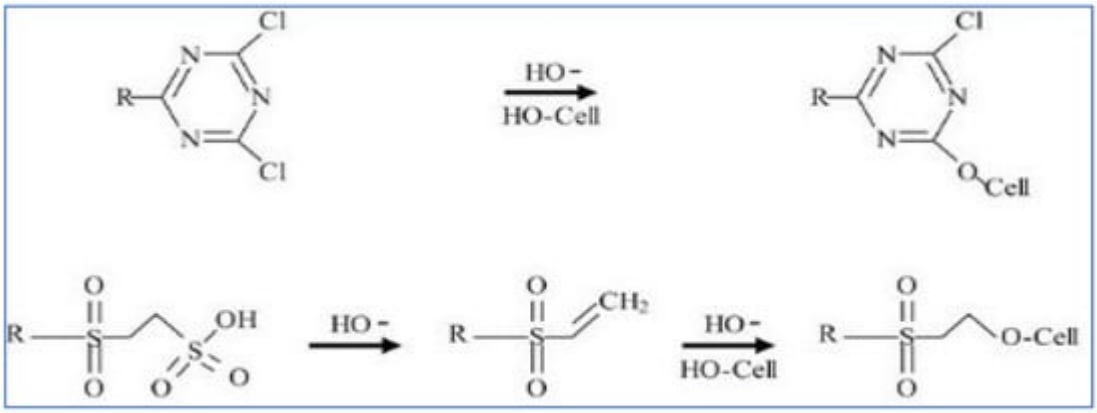

Figure 4. Reactive dyeing mechanism on cellulose.

Due to reactive dyes having a strong bonding affinity for cellulose, consequently, the hydroxyl group containing biosorbents have demonstrated a very strong dye uptake capacity to remove reactive dye compounds from textile dyehouse effluents [14].

2.2. Disperse Dyes

Disperse dyes are non-ionic substances that are commonly applied to polyesters but can be used in acetate or nylon fabrics. These dyes are water soluble and can be used for these fibers by diffusion into the fibers at increased temperatures. As there are no basic chemical groups, there are no attractive sites for acid dye groups, despite a weak attraction for basic dyes. The dye attachment mechanism is based on weak Van der Waals forces and dipole-dipole interactions, implying that like mechanisms may occur during the removal of disperse dyes onto biochar adsorbents [15]. **Figure 5** depicts disperse blue 6 as an example of this class.

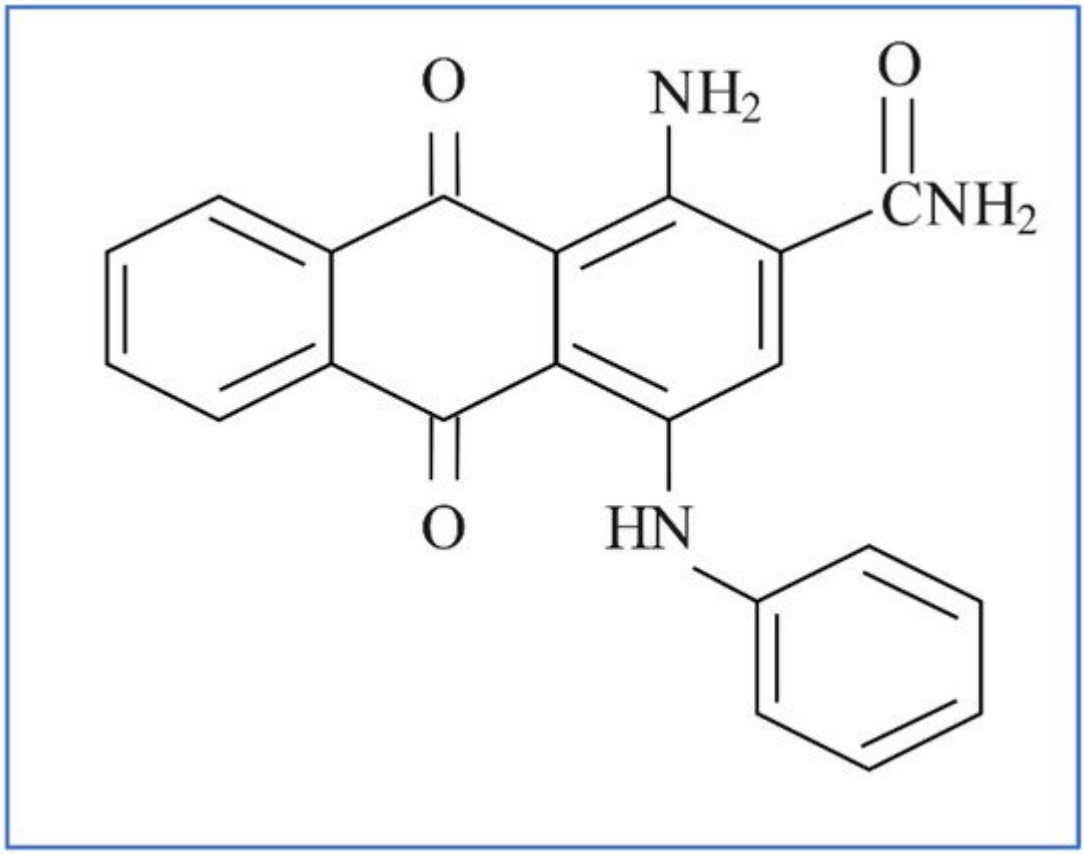

Figure 5. Disperse Blue 6 dye compound.

The dispersed dyestuff occurs typically as a fine suspension that can be filtered from the effluent discharge by biochar.

2.3. Vat Dyes

The majority of vat dyes have a ketonic style chromophore which may be applied to color cellulosic fibers and materials such as viscose, cotton, and linen. This is a broad category of dyes that includes indanthrones, anthraquinones, carbazoles, benzanthrones, polycyclic quinones, and acridones.

Figure 6 shows the structures of a typical vat dye [16].

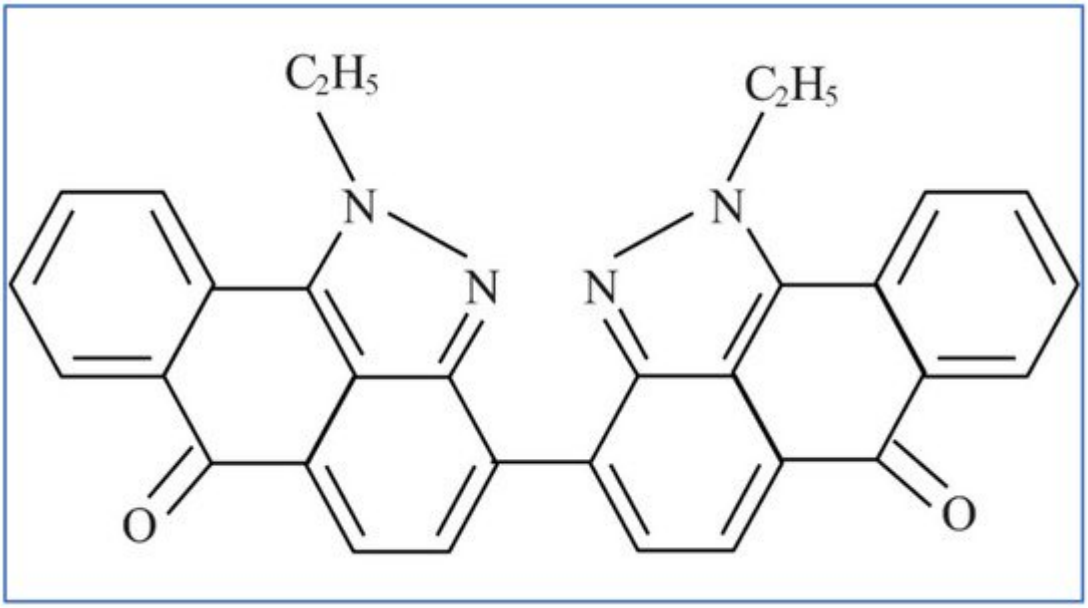

Figure 6. Structure of the vat red 13 dye.

The large anthraquinone groups suggest that the removal process may involve electron clouds of the anthraquinone dye by adsorption onto the positively charged surface groups and adequately sized pore diameters of biochars.

2.4. Direct Dyes

Direct dyes or substantive dyes, as there is no fixation phase necessary, may be applied to color cotton yarn, viscose, and loose cotton of fabrics [17]. Mordant chemicals, such as chromium compounds that can undergo complexation by attaching substrate to chromophore to form an insoluble color, are used in some direct dyes, but not all, to fix the dye and improve color fastness. In the case of dark color shades such as black or navy blue dyes, this technique has proven to be cost-effective in achieving high color fastness. These dyes are now being reviewed due to environment and safety concerns which have limited their use. The mechanism for the application of direct dyes involves establishing non-ionic forces to attach the dyestuff to the textile fiber material [18]. The structure of direct yellow 24 dye is depicted in **Figure 7**.

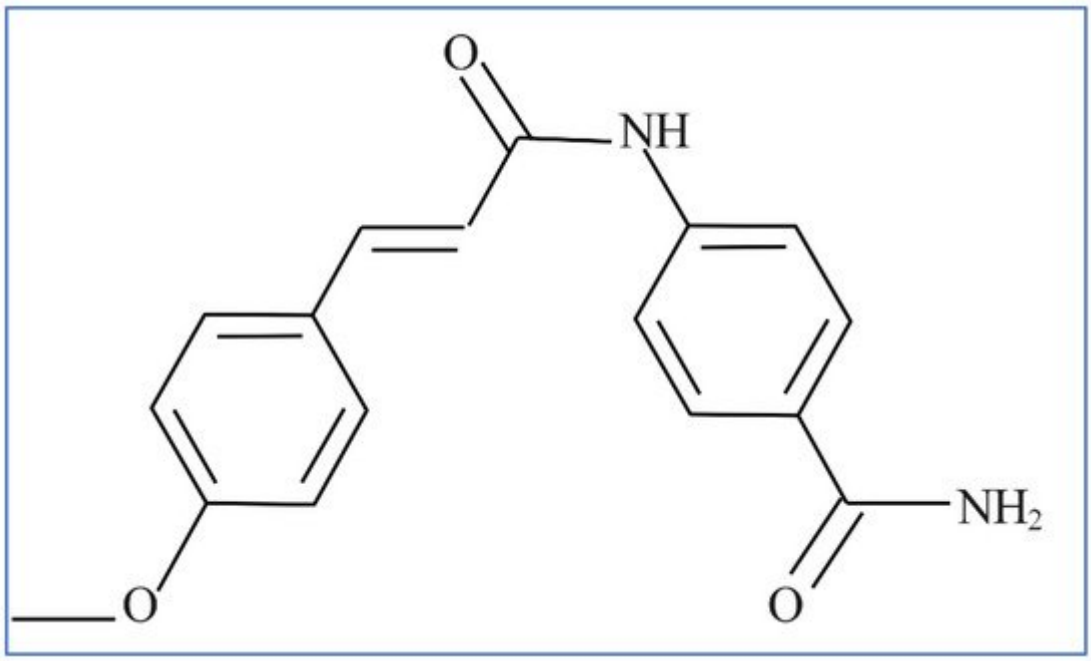

Figure 7. Structure of the direct yellow 24 dye.

Direct dyestuffs produce negatively charged ions in solution and can be adsorbed onto positive sites on biochars.

2.5. Basic Dye

Congo red (CR) is a member of the very large group of basic dyes that are characterized by the color, high tinctorial strength, and brilliance. These basic dyes are most commonly used on acrylic fibers, but they can also be used on other fibrous textiles when mordants are used. Furthermore, basic dyes are soluble media but not soluble in alkaline solutions. These dyes are primarily made up of imino or amino groups that are linked to triarylmethane or xanthene; they are also used in typewriter ribbon, carbon paper, and inks [19]. Monoazo, methane, and oxazine are the three main subclasses. **Figure 8** depicts the structure of a basic CR dye.

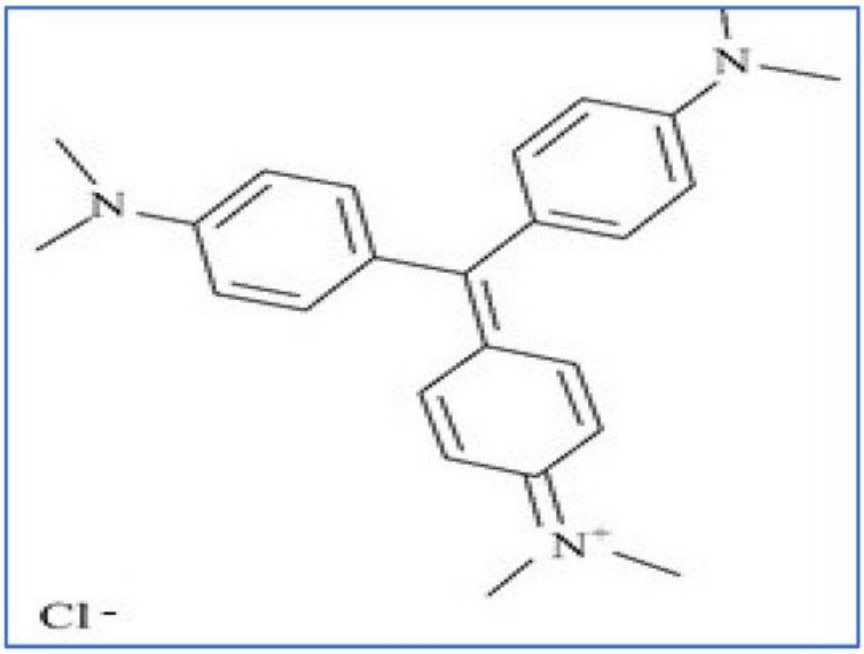

Figure 8. Structure of basic crystal violet (CV) dye.

Since most basic dyes ionize in water, they have a positively charged colored ion or cationic species. These dyes are commonly classified as cationic dyes and adsorb most effectively onto negatively charged functional groups on the biochars [20].

3. Adsorption of Dye onto Biochar Materials for Dye Removal

3.1. Biochar as a Dye Removal Adsorbent

Activated carbons are amorphous carbon-based substances with decent porosity and large internal surface area. Its feedstock can be almost any organic substances with a relatively decent carbon composition, covering traditional materials such as hard and softwood, coconut hull, peat and lignite coal, natural and artificial polymers. Surface areas for marketable carbons typically fall between the 500–1500 m^2/g range [21] and can even reach 3000 m^2/g. Carbon materials are again classified into two sub-categories based on whether they are used to remove pollutant particles from fluids.

The first ones are typically microporous with a pore size of 2 nm diameter and are usually granular, whilst the latter are mesoporous materials with a pore size ranging between 2–50 nm diameter and are usually in powder form [22]. Both types are useful in wastewater treatment, where they aid in decolorization, odor removal, metal recovery, and organics adsorption. The pore volume, internal surface area, and size distribution are all proportional to its adsorption capacity.

Organics have been reported to adsorb in pores just fitting the adsorbate molecule [23]. Humic acids and dyes with size ranging between 1.5 and 3.0 nm that support adsorption phenomenon in mesopores are examples [24]. As a

result, the biochar's pore size dissemination influences its adsorption potential for ions of varying size and shape. The electric strength between the adsorbate and the adsorbent (carbon surface) has proven to improve dye removal efficacy greatly.

The dissociation equilibria and functionality of specific functional sites on biochar material surfaces, such as carboxylic-lactonic groups, phenolic-alcolohic hydroxyl groups, aromatic-heterocyclic carbons, ketone-carbonyl groups, pyridinic-N, pyrollic-N, and quaternary-N nitrogen species, can influence adsorption. These potential biochar surface sites are influenced by several factors, including biomass source, pyrolysis parameters such as heating rate, temperature, residence time, nature of pyrolysis, etc.

Despite that activated and modified carbons are broadly used as adsorbent materials, they are relatively expensive due to the high costs of raw materials, energy, and chemical production. As a result, many researchers have focused on developing novel, high-capacity, low-cost adsorbents obtained from biomass residues. Metal organic frameworks and nano-adsorbent substances have lately been used to create highly efficient adsorbents [25]; however, the cost of treatment renders these materials prohibitively expensive.

As a result, in recent years, several low-cost adsorbents known as biochars have been produced by biomass pyrolysis and used in polluted water treatment applications. The technique is affordable and cost-effective only when the adsorbent is inexpensive and copious [26]. Pyrolysis of biomass leftovers into value-added biochar materials is a cost-effective process that produces high-value-added products: syngas and bio-oil. The pyrolysis process requires energy to run, but the process is driven by the by-products of the side reactions, and biochars possess a larger surface area and pore volume, as well as chemically functional moiety content, making them a much more potent adsorbent material than the biomass feedstock [27][28][29][30].

There are over a thousand papers on color removal in the literature, with over a hundred of these based on dye elimination employing biochar substances, including biochar products derived from vermicompost, cabbage residues, algae, and animal litters [31][32][33][34][35]. There have also been numerous publications on the synthesis and usage of altered biochar materials for dye color elimination. The dye potentials of unmodified/unaltered biochars and others are shown in **Table 1** and **Table 2**.

Table 1 shows the adsorption properties for cationic dye uptake onto unmodified biochars. MG [36][37][38][39][40], MB [41][42][43][44][45][46], rhodamine B (Rh B) [36], basic red 9 (BR 9), and CV [40][47] values are included in the data. Many citations only present the quantity of dye removed (in %) [36][37][41][43][47][48], which is valuable, however, this value varies with adsorbent quantity, dye concentration, and adsorbate volume.

Table 1. Basic dyes (cationic) and their adsorption onto biochars.

Dye	Biochar Feedstock	Pyrolysis Conditions			Pore Volume (cm^3/g)	BET Surface Area (m^2/g)	Adsorption Capacity (mg/g) or Dye Removal (%)	Isotherm Type	Kinetic Model	Parameters		Mechanism	Reference
		Temperature (K)	Heating Rate (K/min)	Time (min)						pH	Equilibrium Time (min)		
MB	Date palm fronds	973	-	240	0.134	430	205	-	-	6	36	-	[41]
MG	Tapioca peel	1073	10	180	-	-	32%	Langmuir, Freundlich	Pseudo I-order, Pseudo-II order	2–10	0–180	-	[36]
Rh B	Tapioca peel	1073	10	180	-	-	66%	Langmuir, Freundlich	Pseudo I-order, Pseudo-II order	2–10	0–180	-	[36]
MB	*Chlorella* sp. *microalgae*	MW heating (2450 MHz, 800 W)	-	-	-	3	110	Freundlich, Temkin	Pseudo I-order, Pseudo-II order, Elovich	2–10	7200	Boyd, Intraparticle diffusion	[42]
MG	Rice husk	673–873	-	60	-	-	65	Langmuir, Freundlich	Pseudo I-order, Pseudo-II order, Elovich	2, 4, 6, 8	1440	-	[37]
MG	Crab shell	1073	-	120	0.086	82	12,500	Langmuir	Pseudo-II order	7	2	Electrostatic attraction, Hydrogen bonding, π-π interactions	[38]
MB	Areca leaf	473	5	60	-	21	120	Langmuir, Freundlich	Pseudo I-order, Pseudo-II order	7	720	Electrostatic attraction	[43]
MB	*Wodyetia Bifurcate*	973	10	30	-	-	150	Sips	Pseudo I-order, Pseudo-II order	-	30	-	[44]
MG	Waste wheat straw/wheat bran	1073	15	90	-	-	1740	Langmuir	Pseudo-II order	2, 4, 6, 8, 10	-	Electrostatic interaction, Chemisorption	[39]

MB adsorption capacities (**Table 1**) are 110, 150, 38, and 195 mg/g for biochar materials derived from microalgae [42], Wodyetia [44], and switchgrass at 873 and 1173 K [23][45], respectively. Pyrolysis temperature significantly influences the adsorption potential of switchgrass biochar. MB adsorption capacity values in the literature for

Dye	Biochar Feedstock	Pyrolysis Conditions			Pore Volume (cm^3/g)	BET Surface Area (m^2/g)	Adsorption Capacity (mg/g) or Dye Removal (%)	Isotherm Type	Kinetic Model	Parameters		Mechanism	Reference
		Temperature (K)	Heating Rate (K/min)	Time (min)						pH	Equilibrium Time (min)		
CV	Waste wheat straw/wheat bran	1073	15	90	-	-	175	Langmuir	Pseudo-II order	2, 4, 6, 8, 10	-	Electrostatic interaction, Chemisorption	[39]
[51]3	Switchgrass [52]	873	-	60	0.[53]	255	40	Langmuir	Pseudo-II order	6	-	Intraparticle diffusion	[45]
MB	Switchgrass-	1173	-	60	0.058	640	200	Langmuir	Pseudo-II order	[36] 6	-	Intraparticle diffusion	[45]
CV	Mango leaves	1073	-	60	-	[54] 170	180		-	8	48	-	[47]
MG	*Ulothrix zonata* algae	1073	15	90	-	130	5300	Freundlich	Pseudo-II order	[55] 2, 4, 6, 10	840	Chemisorption	[40]
CV	*Ulothrix zonata* algae	1073	15	90	-	130	1220	Freundlich	Pseudo-II order	2, 4, 6, 10	840	Chemisorption	[40]
BR 9	Bovine bones	1073	10	60	0.271	90	50	Langmuir, Freundlich	Pseudo-II order	7	180	-	[48]
BR 9	Bovine bones	1073	10	180	0.193	95	50		Pseudo I-order	7	180	-	[48]
MB	Sugarcane bagasse	773	10	90	-	260	70	[58] Langmuir, Freundlich	Pseudo I-order, Pseudo-II order	7.4	[59] 180	Intraparticle diffusion	[46]

Table 2 shows the anionic dye adsorption properties on unmodified biochars. Acid orange 7 (AO 7) [41], CR [33][34][38][39][40][42][45][60][61][62][63], reactive red RR 120 [64], Remazol violet 5R (RV5R), Remazol orange 3R (RO 3R), Remazol blue R (RBR) [65], orange G (OG) [45], and methyl orange (MO) [66] are some of them.

Table 2 shows only the dye removal composition (%) for the adsorption of AO7 using biochar derived from groundnut shell. Only a few instances of AO7 adsorption capacity potential are documented in articles, and they range from 50 to 180 mg/g on fly ash [67], oxihumolite [68], and chemically reactivated sawdust [69].

Table 2. Acid dyes (anionic) and their adsorption onto biochars.

Dye	Biochar Feedstock	Pyrolysis Conditions			Pore Volume (cm^3/g)	BET Surface Area (m^2/g)	Adsorption Capacity (mg/g) or Dye Removal (%)	Isotherm Type	Kinetic Model	Adsorbent Parameters		Mechanism	Reference
		Temperature (K)	Heating Rate (K/min)	Time (min)						pH	Equilibrium Time (min)		
CR	*Chlorella* sp. *microalgal*	MW heating (2450 MHz, 800 W)	-	-	-	3	160	Langmuir, Freundlich, Temkin	Pseudo I-order, Pseudo II-order, Elovich	2–10	240	Boyd, Intraparticle diffusion	[42]
CR	Rice husk	773	5	180	-	-	66–97%	Langmuir, Freundlich	-	2, 4,	5760	-	[34]

Dye	Biochar Feedstock	Pyrolysis Conditions			Pore Volume (cm^3/g)	BET Surface Area (m^2/g)	Adsorption Capacity (mg/g) or Dye Removal (%)	Isotherm Type	Kinetic Model	Adsorbent Parameters		Mechanism	Reference
		Temperature (K)	Heating Rate (K/min)	Time (min)						pH	Equilibrium Time (min)		
										6, 7, 9, 11			
RR 120	*Eucheuma spinosum*	573–873	10	120	-	-	330	Langmuir, Freundlich, Temkin	Pseudo I-order, Pseudo II-order, Elovich	3–9	20	Electrostatic interaction, Ion exchange, Metal complexation, Hydrogen bonding	[64]
CR	*Phoenix dactylifera* leaves	673	-	-	-	1	25	Langmuir, Freundlich	Pseudo I-order, Pseudo II-order	5.8	120	-	[62]
CR	Cotton stalks	673	8	90	-	-	250	Langmuir, Freundlich, Temkin, Dubinin-Radushkevich	Pseudo I-order, Pseudo II-order	2–10	180	Electrostatic attraction	[63]
CR	Orange peel	1073	15	15	-		20		-	-	-	-	[60]
Remazol BV 5R	Green marine algae (*Caulerpa scalpelliformis*)	573–773	5	120	-	-	70%	Langmuir, Freundlich, Sips, T	Pseudo I-order, Pseudo II-order	2–5	-	-	[65]
Remazol BO 3R	Green marine algae (*Caulerpa scalpelliformis*)	573–773	5	120	-	-	77%	Langmuir, Freundlich, Sips, Temkin	Pseudo I-order, Pseudo II-order	2–5	-	-	[65]
Remazol BO 3R	Green marine algae (*Caulerpa scalpelliformis*)	573–773	5	120	-	-	75%	Langmuir, Freundlich, Sips, Temkin	Pseudo I-order, Pseudo II-order	2–5	-	-	[65]
Remazol BO 3R	Crab shell	1073	-	120	0.086	82	20,315	Langmuir	Pseudo I-order, Pseudo II-order	4	2	Electrostatic attraction, Hydrogen bonding, π-π interactions	[38]

As CR is one of the most researched anionic dyestuffs, the citations in **Table 2** are merely illustrative. Adsorption capacity potential of biochars derived from *chlorella* microalgae species [42], *phoenix dactylifera* [62], cotton stalk [63], orange skin [60], carapace (crab shell) [38], activated carbon [61], *spirulina* algae species [33], wheat bran larvae [39], switchgrass (charred at 873 K and 1173 K) [45], and Ulothrix algae species [40] are 160, 25, 250, 90, 20,315, 230, 85, 8, 23, and 345 mg/g. The study on switchgrass indicated that at elevated pyrolysis temperatures, a high-quality biochar is generated.

Most investigations have found that the CR dye adsorption capacity potential is below 100 mg/g. The maximum value was observed from pyrolyzed crab shell with 80 m^2/g surface area. This result was achieved at a pH of 4 and volume to mass ratio of 2; nonetheless, at a CR concentration above 20 g/L. The activated carbon obtained from date stone exhibited a low adsorption capacity potential of 35 mg/g. The huge dye molecular size (695 g/mol) and

Dye	Biochar Feedstock	Pyrolysis Conditions			Pore Volume (cm^3/g) [72]	BET Surface Area (m^2/g)	Adsorption Capacity (mg/g) or Dye Removal (%) [34][71]	Isotherm Type	Kinetic Model	Adsorbent Parameters		Mechanism	Reference
		Temperature (K)	Heating Rate (K/min)	Time (min)						pH	Equilibrium Time (min)		
CR	Activated Carbon	723	20	120	-	-	230	Freundlich	-	2–10	120	-	[61]
CR	Spirulina platensis algae	723	20	120	-	-		Freundlich	-	2–10	120	-	[33]
CR	Waste wheat straw/wheat bran [73]	1073	15	90	-	-	90	Langmuir	Pseudo II-order	2, 4, 6, 8, 10	-	Chemisorption, Electrostatic interaction	[39]
OG	Switchgrass	873	-	60	0.029	255	8	Langmuir	Pseudo II-order	6	-	Outer boundary	[45]
CR	Switchgrass	873	-	60	0.029	255	8	Langmuir	Pseudo II-order	6	-	Outer boundary	[45]
CR	Switchgrass	1173		60	0.058	640	20	Langmuir	Pseudo II-order	6	-	Outer boundary	[45]
CR	*Ulothrix zonata* algae	1073	15	90	-	130	345	Freundlich	Pseudo II-order	2, 4, 6, 10	840	Chemisorption	[40]
MO	Corn cob [64]	873	15	120	-	470	90 [74]	Freundlich	Pseudo II-order	5.6	- [75]	Physiochemical	[66]

yes, is a ore size ctivation lsorption biochars s seen in and 6 h. 33 mg/g. igations' biochars cheuma values in the literature, exhibiting adsorption capacity potentials of 165 and 255 mg/g, respectively. Biochar made from green sea algae [65] has been reported to remove brilliant violet 5R, Remazol, and brilliant orange 3R dyes with removal percentages of more than 70%. On coffee shell activated carbon [76] and calcined eggshell [77], the reported figures for Remazol dyes are relatively low, at 65 and 15 mg/g for brilliant orange 3R and brilliant violet 5R, respectively.

Table 2 demonstrates that biochar derived from switchgrass [45] generated at 873 K displayed a poor orange G adsorption capacity of 8 mg/g. The poor surface area (255 m^2/g) of the char could have contributed to this low capacity. Other published values include 9 mg/g for activated carbon derived from Thespesia populnea [78] and 19 mg/g for nanoporous activated carbon [79]. All of these values indicate that orange G dye is one to be treated. When it came to adsorbing MO, corn cob char [66] had an adsorption capacity potential of 85 mg/g, while amidoxime char [80] had a potential of 140 mg/g.

3.2. Dye Removal Using Adsorption onto Modified Biochars

Several investigations are now being conducted to improve the adsorption efficacy of biochars. Many papers on various biochar modification techniques are available. Treatment or activation of biochar with bases and acids, chemical impregnation, size alteration, and encapsulation are some of the modification techniques. The cationic dye adsorption characteristics and performance properties are shown in **Table 3**.

Table 3. Basic dyes (cationic) and their adsorption onto modified (altered) biochars.

Dye	Modified Biochar Feedstock	Pyrolysis Conditions			Pore Volume (cm^3/g)	BET Surface Area (m^2/g)	Adsorption Capacity (mg/g) or Dye Removal (%)	Isotherm Type	Kinetic Model	Adsorbent Parameters		Mechanism	Reference
		Temperature (K)	Heating Rate (K/min)	Time						pH	Equilibrium Time (min)		
MB	Date palm fronds	1073	20	240	-	70	210	-	-	7	180	-	[81]
MG	Tapioca peel + S- doped	1073	10	180	-	145	30	Langmuir, Freundlich	Pseudo I-order, Pseudo II-order	2–10	1080	-	[36]
Rh B	Tapioca peel + S- doped	1073	10	180	-	145	30	Langmuir, Freundlich	Pseudo I-order, Pseudo II-order	2–10	1080	-	[36]
MB	Areca leaf + $K_2FeO_4^-$	473	5	60	-	20	250	Langmuir, Freundlich	Pseudo I-order, Pseudo II-order	7	720	Electrostatic attraction	[43]
MG	Chitosan-tapioca peel + S-doped	873	-	120	-	120	50	Langmuir, Freundlich	Pseudo I-order, Pseudo II-order	2–12	160	Electrostatic attraction, Hydrogen bonding	[82]
Rh B	Chitosan-tapioca peel + S-doped	873	-	120	-	120	40	Langmuir, Freundlich	Pseudo I-order, Pseudo II-order	2–12	160	Electrostatic attraction, Hydrogen bonding, π-π interactions	[82]
MB	Sugarcane bagasse + steam	1073	10	120	0.356	570	5220	Langmuir, Freundlich	-	7.4	180	-	[83]
MB	Date palm fronds with Fe/Mn	973	3	240	-	430	300	Langmuir, Freundlich	Pseudo I-order, Pseudo II-order, Intraparticle diffusion, Elovich	4–10	240	Surface adsorption, π-π interactions, Ion exchange, Pore-filling	[84]
MB	Wakame *Undaria pinnatifida* leaves with calcination	1073	10	120	-	1160	840	Langmuir, Freundlich	Pseudo I-order, Pseudo II-order	2–12	300	Surface adsorption, Hydrogen bonding, π-π	[85]

Dye	Modified Biochar Feedstock	Pyrolysis Conditions			Pore Volume (cm^3/g)	BET Surface Area (m^2/g)	Adsorption Capacity (mg/g) or Dye Removal (%)	Isotherm Type	Kinetic Model	Adsorbent Parameters		Mechanism	Reference
		Temperature (K)	Heating Rate (K/min)	Time						pH	Equilibrium Time (min)		
												interactions, Pore-filling	
Rh B	Wakame *Undaria pinnatifida* leaves with calcination	1073	10	120	-	1160	530	Langmuir, Freundlich	Pseudo I-order, Pseudo II-order	2–12	300	Surface adsorption, Hydrogen bonding, π-π interactions, Pore-filling	[85]
MG	Wakame *Undaria pinnatifida* leaves with calcination	1073	10	120	-	1160	4065	Langmuir, Freundlich	Pseudo I-order, Pseudo II-order	2–12	300	Surface adsorption, Hydrogen bonding, π-π interactions, Pore-filling	[85]
MG	Corn straw	773	-	180	-	35	520	Langmuir, Freundlich, Temkin	Pseudo I-order, Pseudo II-order, Intra diffusion	2–9	20		[86]
MG	Rice husk + Cu + Al	773	-	60	0.350	200	470	Langmuir, Freundlich		9	200	Pore-filling, π- π interactions	[87]
MG	Litchi peel + HC	1123		60	0.588	1010	2470	Freundlich	Elovich	8	720	Hydrogen bonding, π-π interactions, Pore-filling, Electrostatic interaction	[88]
MG	Sugarcane bagasse + $ZnCl_2$	1073	-	120	0.0235	50	90	Freundlich	Pseudo II-order	8	-	Boyd	[61]

References

1. Akakuru, O.U.; Iqbal, Z.M.; Wu, A. TiO2 Nanoparticles Properties and Applications. In TiO2 Nanoparticles: Applications in Nanobiotechnology and Nanomedicine; John Wiley & Sons, Ltd.: Weinhein, Germany, 2020; pp. 1–66. ISBN 9783527825448.
2. Oyewo, O.A.; Elemike, E.E.; Onwudiwe, D.C.; Onyango, M.S. Metal oxide-cellulose nanocomposites for the removal of toxic metals and dyes from wastewater. Int. J. Biol. Macromol. 2020, 164, 2477–2496.
3. Zhu, S.; Xia, M.; Chu, Y.; Khan, M.A.; Lei, W.; Wang, F.; Muhmood, T.; Wang, A. Adsorption and Desorption of Pb(II) on l-Lysine Modified Montmorillonite and the simulation of Interlayer Structure. Appl. Clay Sci. 2019, 169, 40–47.
4. Khan, S.; Malik, A. Toxicity evaluation of textile effluents and role of native soil bacterium in biodegradation of a textile dye. Environ. Sci. Pollut. Res. 2018, 25, 4446–4458.
5. Kishor, R.; Purchase, D.; Saratale, G.D.; Saratale, R.G.; Ferreira, L.F.R.; Bilal, M.; Chandra, R.; Bharagava, R.N. Ecotoxicological and health concerns of persistent coloring pollutants of textile industry wastewater and treatment approaches for environmental safety. J. Environ. Chem. Eng. 2021, 9, 105012.

6. McKay, G.; Parthasarathy, P.; Sajjad, S.; Saleem, J.; Alherbawi, M. Dye removal using biochars. In Sustainable Biochar for Water and Wastewater Treatment; Mohan, D., Pittman, C.U., E.Mlsna, T., Eds.; Elsevier: Amsterdam, The Netherlands, 2022; pp. 429–471.
7. Forgacs, E.; Cserháti, T.; Oros, G. Removal of synthetic dyes from wastewaters: A review. Environ. Int. 2004, 30, 953–971.
8. Velusamy, S.; Roy, A.; Sundaram, S.; Kumar Mallick, T. A Review on Heavy Metal Ions and Containing Dyes Removal Through Graphene Oxide-Based Adsorption Strategies for Textile Wastewater Treatment. Chem. Rec. 2021, 21, 1570–1610.
9. Global Textile Dyes Industry Report 2015—Forecasts to 2020. Available online: https://www.prnewswire.com/news-releases/global-textile-dyes-industry-report-2015---forecasts-to-2020-498532981.html (accessed on 15 May 2021).
10. Afroze, S.; Sen, T.K. A Review on Heavy Metal Ions and Dye Adsorption from Water by Agricultural Solid Waste Adsorbents. Water Air Soil Pollut. 2018, 229, 1–50.
11. Wang, K.; Wei, T.; Li, Y.; He, L.; Lv, Y.; Chen, L.; Ahmad, A.; Xu, Y.; Shi, Y. Flocculation-to-adsorption transition of novel salt-responsive polyelectrolyte for recycling of highly polluted saline textile effluents. Chem. Eng. J. 2021, 413, 127410.
12. Al-Degs, Y.; Khraisheh MA, M.; Allen, S.J.; Ahmad, M.N. Ahmad Effect of carbon surface chemistry on the removal of reactive dyes from textile effluent. Water Res. 2000, 34, 927–935.
13. Al-Degs, Y.S.; El-Barghouthi, M.I.; El-Sheikh, A.H.; Walker, G.M. Effect of solution pH, ionic strength, and temperature on adsorption behavior of reactive dyes on activated carbon. Dye. Pigment. 2008, 77, 16–23.
14. Chiou, M.S.; Kuo, W.S.; Li, H.Y. Removal of Reactive Dye from Wastewater by Adsorption Using ECH Cross-Linked Chitosan Beads as Medium. J. Environ. Sci. Heal. Part A 2007, 38, 2621–2631.
15. Chakraborty, J.N. Metal complex dyes. In Handbook of Textile and Industrial Dyeing Principles, Processes and Types of Dyes; Clark, M., Ed.; Woodhead Publishing Series in Textiles: Cambridge, UK, 2011; pp. 446–463.
16. Yusuf, A. Vat Dyes-Properties-Dyeing Mechanism-A Comprehensive Look (2020). Available online: https://textiletuts.com/vat-dyes/ (accessed on 2 March 2022).
17. ULLMANN’S Encyclopedia of Industrial Chemistry; Arpe, H.-J. (Ed.) Wiley: Weinheim, Germany, 2000.
18. Asif Tahir, M.; Bhatti, H.N.; Iqbal, M. Solar Red and Brittle Blue direct dyes adsorption onto Eucalyptus angophoroides bark: Equilibrium, kinetics and thermodynamic studies. J. Environ. Chem. Eng. 2016, 4, 2431–2439.

19. Gupta, V.K.; Mohan, D.; Sharma, S.; Sharma, M. Removal of Basic Dyes (Rhodamine B and Methylene Blue) from Aqueous Solutions Using Bagasse Fly Ash. Sep. Sci. Technol. 2007, 35, 2097–2113.
20. Allen, S.J.; Mckay, G.; Porter, J.F. Adsorption isotherm models for basic dye adsorption by peat in single and binary component systems. J. Colloid Interface Sci. 2004, 280, 322–333.
21. Kumar, A.; Balouch, A.; Abdullah. Remediation of toxic fluoride from aqueous media by various techniques. Int. J. Environ. Anal. Chem. 2019, 101, 482–505.
22. Cooney, D. Adsorption Design for Wastewater Treatment; CRC Press; Lewis Publishers: Boca Raton, FL, USA, 1998; ISBN 978-1566703338.
23. Cheremisinoff, P.N. Biomanagement of Wastewater and Wastes; Prentice Hall: New York, NY, USA, 1993.
24. Mui, E.L.K.; Cheung, W.H.; Valix, M.; McKay, G. Dye adsorption onto activated carbons from tyre rubber waste using surface coverage analysis. J. Colloid Interface Sci. 2010, 347, 290–300.
25. Osagie, C.; Othmani, A.; Ghosh, S.; Malloum, A.; Kashitarash Esfahani, Z.; Ahmadi, S. Dyes adsorption from aqueous media through the nanotechnology: A review. J. Mater. Res. Technol. 2021, 14, 2195–2218.
26. Mohan, D.; Sarswat, A.; Ok, Y.S.; Pittman, C.U. Organic and inorganic contaminants removal from water with biochar, a renewable, low cost and sustainable adsorbent—A critical review. Bioresour. Technol. 2014, 160, 191–202.
27. Mui, E.L.K.; Cheung, W.H.; Valix, M.; McKay, G. Dye adsorption onto char from bamboo. J. Hazard. Mater. 2010, 177, 1001–1005.
28. Patel, M.; Kumar, R.; Pittman, C.U.; Mohan, D. Ciprofloxacin and acetaminophen sorption onto banana peel biochars: Environmental and process parameter influences. Environ. Res. 2021, 201, 111218.
29. Vimal, V.; Patel, M.; Mohan, D. Aqueous carbofuran removal using slow pyrolyzed sugarcane bagasse biochar: Equilibrium and fixed-bed studies. RSC Adv. 2019, 9, 26338–26350.
30. Gupta, V.K.; Tyagi, I.; Agarwal, S.; Singh, R.; Chaudhary, M.; Harit, A.; Kushwaha, S. Column operation studies for the removal of dyes and phenols using a low cost adsorbent. Glob. J. Environ. Sci. Manag. 2016, 2, 1–10.
31. Yang, G.; Wu, L.; Xian, Q.; Shen, F.; Wu, J.; Zhang, Y. Removal of Congo Red and Methylene Blue from Aqueous Solutions by Vermicompost-Derived Biochars. PLoS ONE 2016, 11, e0154562.
32. Sewu, D.D.; Boakye, P.; Woo, S.H. Highly efficient adsorption of cationic dye by biochar produced with Korean cabbage waste. Bioresour. Technol. 2017, 224, 206–213.

33. Nautiyal, P.; Subramanian, K.A.; Dastidar, M.G. Adsorptive removal of dye using biochar derived from residual algae after in-situ transesterification: Alternate use of waste of biodiesel industry. J. Environ. Manage. 2016, 182, 187–197.
34. Khan, N.; Chowdhary, P.; Ahmad, A.; Shekher Giri, B.; Chaturvedi, P. Hydrothermal liquefaction of rice husk and cow dung in Mixed-Bed-Rotating Pyrolyzer and application of biochar for dye removal. Bioresour. Technol. 2020, 309, 123294.
35. Huang, W.; Zhang, M.; Wang, Y.; Chen, J.; Zhang, J. Biochars prepared from rabbit manure for the adsorption of rhodamine B and Congo red: Characterisation, kinetics, isotherms and thermodynamic studies. Water Sci. Technol. 2020, 81, 436–444.
36. Vigneshwaran, S.; Sirajudheen, P.; Karthikeyan, P.; Meenakshi, S. Fabrication of sulfur-doped biochar derived from tapioca peel waste with superior adsorption performance for the removal of Malachite green and Rhodamine B dyes. Surfaces Interfaces 2021, 23, 100920.
37. Ganguly, P.; Sarkhel, R.; Das, P. Synthesis of pyrolyzed biochar and its application for dye removal: Batch, kinetic and isotherm with linear and non-linear mathematical analysis. Surfaces Interfaces 2020, 20, 100616.
38. Dai, L.; Zhu, W.; He, L.; Tan, F.; Zhu, N.; Zhou, Q.; He, M.; Hu, G. Calcium-rich biochar from crab shell: An unexpected super adsorbent for dye removal. Bioresour. Technol. 2018, 267, 510–516.
39. Yang, S.S.; Chen, Y.D.; Kang, J.H.; Xie, T.R.; He, L.; Xing, D.F.; Ren, N.Q.; Ho, S.H.; Wu, W.M. Generation of high-efficient biochar for dye adsorption using frass of yellow mealworms (larvae of Tenebrio molitor Linnaeus) fed with wheat straw for insect biomass production. J. Clean. Prod. 2019, 227, 33–47.
40. Di Chen, Y.; Lin, Y.C.; Ho, S.H.; Zhou, Y.; Ren, N. qi Highly efficient adsorption of dyes by biochar derived from pigments-extracted macroalgae pyrolyzed at different temperature. Bioresour. Technol. 2018, 259, 104–110.
41. Zubair, M.; Mu’azu, N.D.; Jarrah, N.; Blaisi, N.I.; Aziz, H.A.; Al-Harthi, A.M. Adsorption Behavior and Mechanism of Methylene Blue, Crystal Violet, Eriochrome Black T, and Methyl Orange Dyes onto Biochar-Derived Date Palm Fronds Waste Produced at Different Pyrolysis Conditions. Water. Air. Soil Pollut. 2020, 231, 1–19.
42. Yu, K.L.; Lee, X.J.; Ong, H.C.; Chen, W.H.; Chang, J.S.; Lin, C.S.; Show, P.L.; Ling, T.C. Adsorptive removal of cationic methylene blue and anionic Congo red dyes using wet-torrefied microalgal biochar: Equilibrium, kinetic and mechanism modeling. Environ. Pollut. 2021, 272, 115986.
43. Yin, Z.; Liu, N.; Bian, S.; Li, J.; Xu, S.; Zhang, Y. Enhancing the adsorption capability of areca leaf biochar for methylene blue by K2FeO4-catalyzed oxidative pyrolysis at low temperature. RSC Adv. 2019, 9, 42343–42350.

44. dos Santos, K.J.L.; dos Santos, G.E.; de Sá, Í.M.G.L.; Ide, A.H.; Duarte, J.L.d.S.; de Carvalho, S.H.V.; Soletti, J.I.; Meili, L. Wodyetia bifurcata biochar for methylene blue removal from aqueous matrix. Bioresour. Technol. 2019, 293, 122093.
45. Park, J.H.; Wang, J.J.; Meng, Y.; Wei, Z.; DeLaune, R.D.; Seo, D.C. Adsorption/desorption behavior of cationic and anionic dyes by biochars prepared at normal and high pyrolysis temperatures. Colloids Surfaces A Physicochem. Eng. Asp. 2019, 572, 274–282.
46. Biswas, S.; Mohapatra, S.S.; Kumari, U.; Meikap, B.C.; Sen, T.K. Batch and continuous closed circuit semi-fluidized bed operation: Removal of MB dye using sugarcane bagasse biochar and alginate composite adsorbents. J. Environ. Chem. Eng. 2020, 8, 103637.
47. Vyavahare, G.; Jadhav, P.; Jadhav, J.; Patil, R.; Aware, C.; Patil, D.; Gophane, A.; Yang, Y.H.; Gurav, R. Strategies for crystal violet dye sorption on biochar derived from mango leaves and evaluation of residual dye toxicity. J. Clean. Prod. 2019, 207, 296–305.
48. Côrtes, L.N.; Druzian, S.P.; Streit, A.F.M.; Godinho, M.; Perondi, D.; Collazzo, G.C.; Oliveira, M.L.S.; Cadaval, T.R.S.; Dotto, G.L. Biochars from animal wastes as alternative materials to treat colored effluents containing basic red 9. J. Environ. Chem. Eng. 2019, 7, 103446.
49. Lafi, W.K. Production of activated carbon from acorns and olive seeds. Biomass Bioenergy 2001, 20, 57–62.
50. Hameed, B.H.; Din, A.T.M.; Ahmad, A.L. Adsorption of methylene blue onto bamboo-based activated carbon: Kinetics and equilibrium studies. J. Hazard. Mater. 2007, 141, 819–825.
51. Sayğili, H.; Güzel, F. Performance of new mesoporous carbon sorbent prepared from grape industrial processing wastes for malachite green and congo red removal. Chem. Eng. Res. Des. 2015, 100, 27–38.
52. Salamat, S.; Hadavifar, M.; Rezaei, H. Preparation of nanochitosan-STP from shrimp shell and its application in removing of malachite green from aqueous solutions. J. Environ. Chem. Eng. 2019, 7, 103328.
53. Li, Z.; Chen, K.; Chen, Z.; Li, W.; Biney, B.W.; Guo, A.; Liu, D. Removal of malachite green dye from aqueous solution by adsorbents derived from polyurethane plastic waste. J. Environ. Chem. Eng. 2021, 9, 104704.
54. Danish, M.; Ahmad, T.; Hashim, R.; Said, N.; Akhtar, M.N.; Mohamad-Saleh, J.; Sulaiman, O. Comparison of surface properties of wood biomass activated carbons and their application against rhodamine B and methylene blue dye. Surfaces Interfaces 2018, 11, 1–13.
55. Da Silva Lacerda, V.; López-Sotelo, J.B.; Correa-Guimarães, A.; Hernández-Navarro, S.; Sánchez-Báscones, M.; Navas-Gracia, L.M.; Martín-Ramos, P.; Martín-Gil, J. Rhodamine B removal with activated carbons obtained from lignocellulosic waste. J. Environ. Manage. 2015, 155, 67–76.

56. Fabryanty, R.; Valencia, C.; Soetaredjo, F.E.; Putro, J.N.; Santoso, S.P.; Kurniawan, A.; Ju, Y.H.; Ismadji, S. Removal of crystal violet dye by adsorption using bentonite—alginate composite. J. Environ. Chem. Eng. 2017, 5, 5677–5687.

57. Pal, A.; Pan, S.; Saha, S. Synergistically improved adsorption of anionic surfactant and crystal violet on chitosan hydrogel beads. Chem. Eng. J. 2013, 217, 426–434.

58. Duman, O.; Tunç, S.; Gürkan Polat, T. Adsorptive removal of triarylmethane dye (Basic Red 9) from aqueous solution by sepiolite as effective and low-cost adsorbent. Microporous Mesoporous Mater. 2015, 210, 176–184.

59. Kizilkaya, B. Usage of Biogenic Apatite (Fish Bones) on Removal of Basic Fuchsin Dye from Aqueous Solution. J. Dispers. Sci. Technol. 2012, 33, 1596–1602.

60. Yek, P.N.Y.; Peng, W.; Wong, C.C.; Liew, R.K.; Ho, Y.L.; Wan Mahari, W.A.; Azwar, E.; Yuan, T.Q.; Tabatabaei, M.; Aghbashlo, M.; et al. Engineered biochar via microwave CO2 and steam pyrolysis to treat carcinogenic Congo red dye. J. Hazard. Mater. 2020, 395, 122636.

61. Das, L.; Sengupta, S.; Das, P.; Bhowal, A.; Bhattacharjee, C. Experimental and Numerical modeling on dye adsorption using pyrolyzed mesoporous biochar in Batch and fixed-bed column reactor: Isotherm, Thermodynamics, Mass transfer, Kinetic analysis. Surfaces Interfaces 2021, 23, 100985.

62. Iqbal, J.; Shah, N.S.; Sayed, M.; Niazi, N.K.; Imran, M.; Khan, J.A.; Khan, Z.U.H.; Hussien, A.G.S.; Polychronopoulou, K.; Howari, F. Nano-zerovalent manganese/biochar composite for the adsorptive and oxidative removal of Congo-red dye from aqueous solutions. J. Hazard. Mater. 2021, 403, 123854.

63. Iqbal, M.M.; Imran, M.; Hussain, T.; Naeem, M.A.; Al-Kahtani, A.A.; Shah, G.M.; Ahmad, S.; Farooq, A.; Rizwan, M.; Majeed, A.; et al. Effective sequestration of Congo red dye with ZnO/cotton stalks biochar nanocomposite: MODELING, reusability and stability. J. Saudi Chem. Soc. 2021, 25, 101176.

64. Gurav, R.; Bhatia, S.K.; Choi, T.R.; Choi, Y.K.; Kim, H.J.; Song, H.S.; Lee, S.M.; Lee Park, S.; Lee, H.S.; Koh, J.; et al. Application of macroalgal biomass derived biochar and bioelectrochemical system with Shewanella for the adsorptive removal and biodegradation of toxic azo dye. Chemosphere 2021, 264, 128539.

65. Gokulan, R.; Avinash, A.; Prabhu, G.G.; Jegan, J. Remediation of remazol dyes by biochar derived from Caulerpa scalpelliformis—An eco-friendly approach. J. Environ. Chem. Eng. 2019, 7, 103297.

66. Zhang, Z.; Wang, G.; Li, W.; Zhang, L.; Chen, T.; Ding, L. Degradation of methyl orange through hydroxyl radical generated by optically excited biochar: Performance and mechanism. Colloids Surfaces A Physicochem. Eng. Asp. 2020, 601, 125034.

67. Janoš, P.; Buchtová, H.; Rýznarová, M. Sorption of dyes from aqueous solutions onto fly ash. Water Res. 2003, 37, 4938–4944.
68. Janoš, P.; Šedivý, P.; Rýznarová, M.; Grötschelová, S. Sorption of basic and acid dyes from aqueous solutions onto oxihumolite. Chemosphere 2005, 59, 881–886.
69. Janoš, P.; Coskun, S.; Pilařová, V.; Rejnek, J. Removal of basic (Methylene Blue) and acid (Egacid Orange) dyes from waters by sorption on chemically treated wood shavings. Bioresour. Technol. 2009, 100, 1450–1453.
70. Bouhemal, N.; Addoun, F. Adsorption of dyes from aqueous solution onto activated carbons prepared from date pits: The effect of adsorbents pore size distribution. Desalin. Water Treat. 2009, 7, 242–250.
71. Bouchemal, N.; Azoudj, Y.; Merzougui, Z.; Addoun, F. Adsorption modeling of orange G dye on mesoporous activated carbon prepared from algerian date pits using experimental designs. Desalin. Water Treat. 2012, 45, 284–290.
72. Li, Y.; Meas, A.; Shan, S.; Yang, R.; Gai, X. Production and optimization of bamboo hydrochars for adsorption of Congo red and 2-naphthol. Bioresour. Technol. 2016, 207, 379–386.
73. Li, C.; Zhang, L.; Xia, H.; Peng, J.; Zhang, S.; Cheng, S.; Shu, J. Kinetics and isotherms studies for congo red adsorption on mesoporous Eupatorium adenophorum-based activated carbon via microwave-induced H3PO4 activation. J. Mol. Liq. 2016, 224, 737–744.
74. Absalan, G.; Asadi, M.; Kamran, S.; Sheikhian, L.; Goltz, D.M. Removal of reactive red-120 and 4-(2-pyridylazo) resorcinol from aqueous samples by Fe3O4 magnetic nanoparticles using ionic liquid as modifier. J. Hazard. Mater. 2011, 192, 476–484.
75. Oueslati, K.; Lima, E.C.; Ayachi, F.; Cunha, M.R.; Ben Lamine, A. Modeling the removal of Reactive Red 120 dye from aqueous effluents by activated carbon. Water Sci. Technol. 2020, 82, 651–662.
76. Ahmad, M.A.; Rahman, N.K. Equilibrium, kinetics and thermodynamic of Remazol Brilliant Orange 3R dye adsorption on coffee husk-based activated carbon. Chem. Eng. J. 2011, 170, 154–161.
77. Rápó, E.; Posta, K.; Suciu, M.; Szép, R.; Tonk, S. Adsorptive Removal of Remazol Brilliant Violet-5R Dye from Aqueous Solutions using Calcined Eggshell as Biosorbent. Acta Chim. Slov. 2019, 66, 648–658.
78. Arulkumar, M.; Sathishkumar, P.; Palvannan, T. Optimization of Orange G dye adsorption by activated carbon of Thespesia populnea pods using response surface method-ology. J. Hazard. Mater. 2011, 186, 827–834.
79. Kundu, S.; Chowdhury, I.H.; Naskar, M. Synthesis of hexagonal shaped nanoporous carbon for efficient adsorption of methyl orange dye. J. Mol. Liq. 2017, 234, 417–423.

80. Rahman, N.; Dafader, N.C.; Miah, A.R.; Shahnaz, S. Efficient removal of methyl orange from aqueous solution using amidoxime adsorbent. Int. J. Environ. Stud. 2018, 76, 594–607.
81. Ghany, H.M.A. Production of a new activated carbon prepared from palm fronds by thermal activation. Int. J. Eng. Technol. Manag. Res. 2019, 6, 34–43.
82. Vigneshwaran, S.; Sirajudheen, P.; Nikitha, M.; Ramkumar, K.; Meenakshi, S. Facile synthesis of sulfur-doped chitosan/biochar derived from tapioca peel for the removal of organic dyes: Isotherm, kinetics and mechanisms. J. Mol. Liq. 2021, 326, 115303.
83. Carrier, M.; Hardie, A.G.; Uras, Ü.; Görgens, J.; Knoetze, J. Production of char from vacuum pyrolysis of South-African sugar cane bagasse and its characterization as activated carbon and biochar. J. Anal. Appl. Pyrolysis 2012, 96, 24–32.
84. Zubair, M.; Manzar, M.S.; Mu’azu, N.D.; Anil, I.; Blaisi, N.I.; Al-Harthi, M.A. Functionalized MgAl-layered hydroxide intercalated date-palm biochar for Enhanced Uptake of Cationic dye: Kinetics, isotherm and thermodynamic studies. Appl. Clay Sci. 2020, 190, 105587.
85. Yao, X.; Ji, L.; Guo, J.; Ge, S.; Lu, W.; Chen, Y.; Cai, L.; Wang, Y.; Song, W. An abundant porous biochar material derived from wakame (Undaria pinnatifida) with high adsorption performance for three organic dyes. Bioresour. Technol. 2020, 318, 124082.
86. Yang, R.T. Adsorbents: Fundamentals and Applications; John Wiley & Sons: New York, NY, USA, 2003; ISBN 9780471297413.
87. Palapa, N.R.; Taher, T.; Rahayu, B.R.; Mohadi, R.; Rachmat, A.; Lesbani, A. CuAl LDH/Rice husk biochar composite for enhanced adsorptive removal of cationic dye from aqueous solution. Bull. Chem. React. Eng. Catal. 2020, 15, 525–537.
88. Wu, J.; Yang, J.; Feng, P.; Huang, G.; Xu, C.; Lin, B. High-efficiency removal of dyes from wastewater by fully recycling litchi peel biochar. Chemosphere 2020, 246, 125734.
89. Tsai, W.T.; Chen, H.R. Removal of malachite green from aqueous solution using low-cost chlorella-based biomass. J. Hazard. Mater. 2010, 175, 844–849.